Applied Mathematics and Computation 432 (2022) 127365

Contents lists available at ScienceDirect

Applied Mathematics and Computation

journal homepage: www.elsevier.com/locate/amc

Investigating the trade-off between self-quarantine and forced quarantine provisions to control an epidemic: An evolutionary approach

Md. Mamun-Ur-Rashid Khan [a,c,*], Md. Rajib Arefin [a,c], Jun Tanimoto [a,b]

[a] Interdisciplinary Graduate School of Engineering Sciences, Kyushu University, Kasuga-koen, Kasuga-shi, Fukuoka 816-8580, Japan
[b] Faculty of Engineering Sciences, Kyushu University, Kasuga-koen, Kasuga-shi, Fukuoka 816-8580, Japan
[c] Department of Mathematics, University of Dhaka, Dhaka 1000, Bangladesh

ARTICLE INFO

Article history:
Received 18 April 2022
Revised 19 June 2022
Accepted 26 June 2022
Available online 6 July 2022

Keywords:
Self-quarantine
Behavior dynamics
Forced quarantine
Critical line
Social efficiency deficit

ABSTRACT

During a pandemic event like the present COVID-19, self-quarantine, mask-wearing, hygiene maintenance, isolation, forced quarantine, and social distancing are the most effective nonpharmaceutical measures to control the epidemic when the vaccination and proper treatments are absent. In this study, we proposed an epidemiological model based on the SEIR dynamics along with the two interventions defined as self-quarantine and forced quarantine by human behavior dynamics. We consider a disease spreading through a population where some people can choose the self-quarantine option of paying some costs and be safer than the remaining ones. The remaining ones act normally and send to forced quarantine by the government if they get infected and symptomatic. The government pays the forced quarantine costs for individuals, and the government has a budget limit to treat the infected ones. Each intervention derived from the so-called behavior model has a dynamical equation that accounts for a proper balance between the costs for each case, the total budget, and the risk of infection. We show that the infection peak cannot be reduced if the authority does not enforce a proactive (quantified by a higher sensitivity parameter) intervention. While comparing the impact of both self- and forced quarantine provisions, our results demonstrate that the latter is more influential to reduce the disease prevalence and the social efficiency deficit (a gap between social optimum payoff and equilibrium payoff).

1. Introduction

Quarantine, lockdowns, and other distancing restrictions may be the only way to stop a pandemic from spreading, especially if there are no vaccinations or proper medications available to treat the symptoms of infection [1–15]. Epidemiologists and other professionals usually define these social principles but putting them into practice can be very difficult [9,16]. Despite evidence of prospective concerns, the current COVID-19 situation reveals how certain people are more prone to self-isolation under voluntary quarantine than others. Individuals who refuse to accept any type of limitation put themselves and their communities at risk. In these situations, knowing how to encourage and maintain prosocial behavior is crucial [9].

* Corresponding author.
E-mail address: mamun.math@du.ac.bd (Md.M. Khan).

https://doi.org/10.1016/j.amc.2022.127365

In this study, we examine the impact of individual quarantine preferences and government-imposed quarantine on epidemic dynamics. We model individual's decision to commit self-quarantine based on the overall scenario, including the number of infected people, self-quarantine cost, and self-quarantine effort, as well as the government's decision to maintain the forced quarantine based on the forced quarantine cost, total budget, and number of infected peoples, using evolutionary game theory (EGT) [17–19].

Currently, sustaining self-quarantine by individuals and compulsory quarantine by the government are the two most powerful control strategies against the transmission of SARS-CoV2 during this COVID-19 epidemic [20–23]. There are substantial disagreements among people in various locations about maintaining self-quarantine, particularly in low-income countries where everyone cannot pay the cost of self-quarantine because of economic constraints. However, in many nations, the government has funding constraints, space constraints, healthcare personnel and instrumentation constraints when caring for diseased people. These behavioral treatments have already demonstrated their value in studying the interaction between illnesses and human decision-making in the context of social dilemmas [24–30].

Compartmental models, common tool in epidemiology and current health management systems, are widely used to investigate a pandemic or epidemic process [1,6,7,9,11,15,18,26,29–37]. One of the most widely used epidemiological models is the SIR model [32,38,39]. It shows how illness spreads in agents from the susceptible compartment, S, to the infectious compartment, I, and finally to the recovered (or eliminated) compartment R, imparting immunity against re-infection [9]. It has been widely used to retrieve relevant parts of epidemic processes that have the SIR structure despite its simplicity [9,34,38–41]. Since its creation by Kermack and McKendrick, the model has been thoroughly explored and expanded to meet a variety of hypotheses and situations [9]. Some epidemics, for example, may demand the addition of additional compartments, such as those harboring exposed, asymptomatic agents, Quarantined agents, Hospitalized agents (known as SEIR, SEAIR, SEIAQR, SEIAQHR models respectively) [9,42–45]. Other applications for compartmental models in epidemiology include the investigation of control and mitigation techniques such as vaccination, the modeling of vector-borne diseases, and the effects of birth and death dynamics [9,39]. Even the propagation of misinformation and corruption has found a natural home in the SIR model [9]. However, most of these models focus solely on illness progression, with agents doing no conscious activities in relation to the condition [9]. Meanwhile, many infectious diseases control techniques rely on individual decision-making. In this setting, the new discipline of behavioral epidemiology [9,39,42,46,47], which applies psychology, game theory approaches to epidemiology, has attracted significant attention. Behavioral epidemiology considers dynamic behavior changes instead of static roles for agents. This is ideal ground for the new field of social dynamics or sociophysics, which combines statistical physics tools with evolutionary game theory (and other approaches) to better understand human behavior [9,17]. For example, Bauch used a unique way to examine vaccination decision dynamics by including a SIR model into an EGT framework [46,47]. Agents adjust their vaccination strategy dynamically because of this based on their perceptions of the vaccine's advantages and costs. This was eventually developed into the framework of "vaccination games" [24,46,48–51]. As a result of this technique, several intriguing observations and predictions in vaccination procedures have been made. Unfortunately, vaccination is not always an option, and social isolation may be the only method to keep the disease from spreading further. This was true during the Spanish flu, the SARS epidemic of 2002–2003, and most recently, the COVID-19 pandemic [9,52–53].

We modeled the epidemic formulation using the epidemic technique, where the population is initially divided into two divisions: committing self-quarantine and acting normally. From a game-theoretical perspective, individuals can go from the normal active state to the self-quarantine state based on their choices. Similarly, the government can send symptomatic sick people to a forced quarantine condition. EGT provides a framework for describing individual behavior in situations where people's preferred options are committing self-quarantine or not, as well as being sent to coercive quarantine or not. We also used the cost of individuals' self-quarantine, cost of individuals' forced quarantine, and overall government expenditure in this study. Finally, to get the social dilemma in EGT, the model introduces the concept of social efficiency deficit (SED), which is the difference between Nash equilibrium (NE) and social optimum (SO) [1,8,24,29–30].

2. Model description

2.1. Epidemiological model

We propose an epidemiological model based on the SEIR dynamics. We also introduce two behaviors known as self-quarantine by individuals and forced quarantine by the government. Fig. 1 shows the schematic of the proposed model, and the formulation is given as follows:

$$\frac{dS_N(t)}{dt} = -S_N \cdot (\beta_N \cdot (\varepsilon_I \cdot I_A(t) + I_S(t) + \varepsilon_Q \cdot Q(t))) - x(t) \ . \ S_N(t) \tag{1.1}$$

$$\frac{dS_Q(t)}{dt} = -S_Q \cdot (\beta_Q \cdot (\varepsilon_I \cdot I_A(t) + I_S(t) + \varepsilon_Q \cdot Q(t))) + x(t) \ . \ S_N(t) \tag{1.2}$$

$$\frac{dE(t)}{dt} = S_N \cdot (\beta_N \cdot (\varepsilon_I \cdot I_A(t) + I_S(t) + \varepsilon_Q \cdot Q(t))) + S_Q \cdot (\beta_Q \cdot (\varepsilon_I \cdot I_A(t) + I_S(t) + \varepsilon_Q \cdot Q(t))) - \sigma \cdot E(t) \tag{1.3}$$

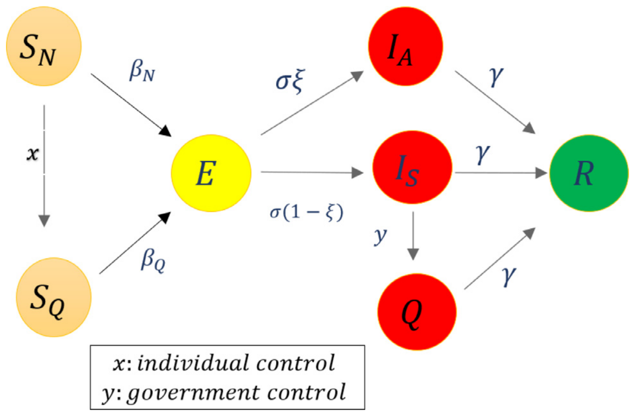

Fig. 1. Schematic of the proposed model.

$$\frac{dI_A(t)}{dt} = \xi \cdot \sigma \cdot E(t) - \gamma \cdot I_A(t) \tag{1.4}$$

$$\frac{dI_S(t)}{dt} = (1-\xi) \cdot \sigma \cdot E(t) - \gamma \cdot I_S(t) - y(t) \cdot I_S(t) \tag{1.5}$$

$$\frac{dQ(t)}{dt} = y(t) \cdot I_S(t) - \gamma \cdot Q(t) \tag{1.6}$$

$$\frac{dR(t)}{dt} = \gamma \cdot (I_A(t) + I_S(t) + Q(t)) \tag{1.7}$$

$$S_N(t) + S_Q(t) + E(t) + I_A(t) + I_S(t) + Q(t) + R(t) = 1 \tag{1.8}$$

where, $S_N, S_Q, E,\ I_A, I_S, Q,$ and R are the fractions of susceptible acting normal, susceptible self-quarantine, exposed (i.e., infected but not infectious), asymptomatic infected, symptomatic infected, forced quarantine, and recovered individuals, respectively. Susceptible normal people get exposed at a rate of β_N, and susceptible people commit self-quarantine getting exposed at a rate of β_Q. Clearly, $\beta_N > \beta_Q$. At a rate ξ, the exposed people go to the asymptomatic infected state. In our model, we choose the asymptomatic infected people quite low than the symptomatic infected people. γ is the recovered rate for all people. σ is the rate of progression from E to I_A or I_S. ε_I and ε_Q are the contact discount factors for the asymptomatic infected people and forced quarantined people, respectively. Obviously, $\varepsilon_I > \varepsilon_Q \approx 0$, because people get infected having contacts with the asymptomatic people while people are not getting chance to contact with the forced quarantined people due to the quarantine policy. The contact discount factor for the symptomatic infected people is set at 1 because people always get infected having contact with symptomatic people.

2.2. Behavior model

We introduce the concept of behavior model [46,47,54] which accounts for the time-varying flux from normal acting susceptible (S_N) to self-quarantine susceptible (S_Q) denoted by x, which we call the individual control, and from the symptomatic infected (I_S) to forced quarantine (Q) denoted by y, which we call the government control. We define the following two dynamical equations:

$$\frac{dx(t)}{dt} = \tau_x \cdot x(t) \cdot (1-x(t)) \cdot [(I_S + Q) \cdot C_I - w.\ \Delta_Q] \tag{1.9}$$

$$\frac{dy(t)}{dt} = \tau_y \cdot y(t) \cdot (1-y(t)) \cdot \left[A_p - \left(\delta_{I_S+Q}\right) \cdot \int_0^t y(\tau)d\tau\right] \tag{1.10}$$

where τ_x and τ_y are the effort rate by individual and government, respectively. $(I_S + Q)$ is the total visible infected people, C_I is the diseases cost which is set as 1.0 throughout the study. Parameter w is the relative sensitivity resulting from taking self-quarantine to reduce self-quarantine due to its cost Δ_Q [54]. δ_{I_S+Q} is the cost for an individual to treat the forced quarantine people. A_P is the government total budget for the treatment of the forced quarantine people. All the model parameters and their description are shown in Table 1.

We also investigated the possibility of susceptible self-quarantined people returning to their susceptible normal behaving state [31], but the results were similar using both directions with one direction. We only investigated the one-way direction from susceptible normal to susceptible self-quarantine.

Table 1
List of parameters and their description.

Parameters	Description
β_N	Disease Transmission rate from S_N
β_Q	Disease Transmission rate from S_Q
σ	Rate of progression from E to I_A or I_S
ξ	Asymptomatic infection rate
γ	Recovery rate
τ_x	Self-quarantine effort rate
τ_y	Forced quarantine effort rate
Δ_Q	Self-quarantine cost for individual
ε_I	Contact discount factor for asymptomatic people
ε_Q	Contact discount factor for forced quarantine people
A_p	Government total budget (resource)
δ_{I_S+Q}	Forced quarantine cost for individual
w	Relative sensitivity due to individual's self-quarantine cost

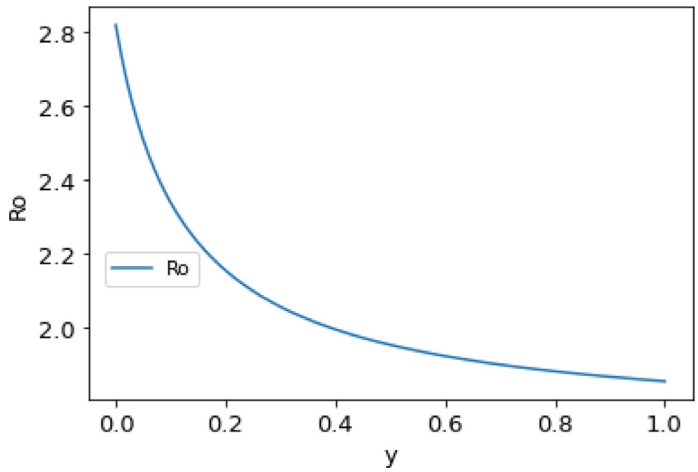

Fig. 2. Basic reproduction Number (1.11) in terms of forced quarantine rate y. Here, $S_{N_0}=0.9887,\ \beta_N=1.0,\ S_{Q_0}=0.01,\ \beta_Q=0.5,\ \gamma=0.1,\ \varepsilon_I=0.6,\ \xi=0.1$. With the increasing y from 0 to 1, R_0 reduces to 2.82 to 1.85.

2.3. Basic reproduction number

To obtain the basic reproduction number (R_0), we use the next-generation matrix approach [31,38,39,42,55,56]. Using the infected class Eqs. (1.3–1.5), we obtain

$$\mathcal{F}=\begin{pmatrix}(S_N\beta_N\varepsilon_I+S_Q\beta_Q\varepsilon_I)I_A+(S_N\beta_N+S_Q\beta_Q)I_S+(S_N\beta_N\varepsilon_Q+S_Q\beta_Q\varepsilon_Q)Q\\ \xi\sigma E\\ (1-\xi)\sigma E\end{pmatrix},\quad \nu=\begin{pmatrix}\sigma E\\ \gamma I_A\\ (\gamma+y)I_S\end{pmatrix}$$

At disease free equilibrium (DFE), we have

$$F=\begin{pmatrix}0 & (S_{N_0}\beta_N\varepsilon_I+S_{Q_0}\beta_Q\varepsilon_I) & (S_{N_0}\beta_N+S_{Q_0}\beta_Q)\\ \xi\sigma & 0 & 0\\ \sigma(1-\xi) & 0 & 0\end{pmatrix},\quad V=\begin{pmatrix}\sigma & 0 & 0\\ 0 & \gamma & 0\\ 0 & 0 & \gamma+y\end{pmatrix}.$$

Next-generation matrix, $M=FV^{-1}=\begin{pmatrix}0 & \frac{(S_{N_0}\beta_N\varepsilon_I+S_{Q_0}\beta_Q\varepsilon_I)}{\gamma} & \frac{(S_{N_0}\beta_N+S_{Q_0}\beta_Q)}{\gamma+y}\\ \xi & 0 & 0\\ (1-\xi) & 0 & 0\end{pmatrix}.$

Thus, we obtain the basic reproduction number as follows:

$$R_0=\sqrt{\frac{S_{N_0}\beta_N+S_{Q_0}\beta_Q}{\gamma+y}(1-\xi)+\xi\frac{S_{N_0}\beta_N\varepsilon_I+S_{Q_0}\beta_Q\varepsilon_I}{\gamma}} \tag{1.11}$$

at DFE $=(S_{N_0},S_{Q_0},0,0,0,0,0)$.

The basic reproduction number in our model decreases monotonically with increase in y because it depends on the factors and governments control flux y (Fig. 2).

Table 2
Parameters and their values (Standard case).

Parameter	Value	Parameter	Value
β_N	1.0	τ_y	1.0
β_Q	0.5	Δ_Q, δ_{I_S+Q}	0.01
σ	0.9	ε_I	0.6
ξ	0.1	ε_Q	0.0
γ	0.1	A_p	1.0
τ_x	1.0	w	0.1

2.4. Final Epidemic size, critical point, average social payoff, and social efficiency deficit

In the present model, final epidemic size (FES) [42,54] is defined as

$$FES = R(\infty) \tag{1.12}$$

where the argument ∞ denotes a state of equilibrium (let us call it as, NE) at $t = \infty$ [54].

We also define the difference of FES between without interventions and with those:

$$\Delta FES = \text{FES(No intervention)} - \text{FES(with both interventions)} \tag{1.13}$$

ΔFES is mainly controlled by Δ_Q and δ_{I_S+Q}. One interesting exploration is the analysis on critical points $(\Delta_Q, \delta_{I_S+Q})$ such that the reduced cost by both interventions, i.e., exactly quantified by ΔFES, is stringently equal to the sum of the total self-quarantine cost and total forced quarantine cost, i.e.,

$$\Delta FES = \text{Total self quarantine cost (at t} = \infty) + \text{Total forced quarantine cost (at t} = \infty) \tag{1.14}$$

Average social payoff, $\mathrm{ASP^{NE}}$, in the model can be defined as follows [54]:

$$ASP^{NE} = (-\Delta_Q) \cdot \int_0^\infty x(t) \cdot \; S_N(t) \; dt + \left(-\delta_{I_S+Q}\right) \cdot \int_0^\infty y(t) \cdot \; I_S(t) \; dt - C_I \cdot \; R(\infty) \tag{1.15}$$

where the first term in the right-hand side indicates the total cost of committing self-quarantine, the second term indicates the total cost of the implementation of forced quarantine, and the third term indicates the individuals' diseases cost ($C_I = 1.0$) who should be called as a failed free rider [54].

Since the rates of self- and forced quarantine provisions change over time according to the behavior dynamics (Eq. (1.9-1.10)), the overall social gain estimated at the equilibrium (i.e., ASP^{NE} in Eq. (1.15)) may not reach the expected social optimum (say, $\mathrm{ASP^{SO}}$). In other words, there might be a gap between the overall payoffs at social optimum and at equilibrium. Such a gap is formally called social efficiency deficit (SED) [29], which helps us understand the existence of social dilemma as well as the control parameters to improve the system towards social optimum. SED demonstrates how to improve the system's ASP from an evolutionary final state (NE) to a social ideal situation in order to achieve the maximum $\mathrm{ASP^{SO}}$ that could be realized if both the evolutionary processes for x and y are optimally controlled [54]. SED is mathematically defined as follows:

$$SED = ASP^{SO} - ASP^{NE} \tag{1.16}$$

The social optimal state can be defined as a time-constant vector $(x^{for\,SO}, y^{for\,SO})$, both elements ranging from [0, 1]. So,

$$\boldsymbol{SO} = \arg\max\left[ASP\left(x^{for\ SO}, y^{for\ SO}\right)\right] \tag{1.17}$$

There is no dilemma when NE is consistent with SO, meaning that SED implies zero. However, when a positive nonzero SED occurs, a certain amount of social dilemma exists [54].

3. Result and discussion

3.1. Standard (Basic) case

Fig. 3 shows the time-series graph using the standard (basic) set of parameters for the proposed model. Table 2 shows the standard values of the parameters.

Additionally, the initial values for the compartments are considered as: $S_N[0] = 0.9887$, $S_Q[0] = 0.01$, $E[0] = 0.0001$, $I_A[0] = 0.001$, $I_S[0] = 0.0001$, $Q[0] = 0.0001$, $R[0] = 0.0$, $x[0] = 0.0001$, $y[0] = 0.0001$.

Fig. 3 confirms the present model fairly shows plausible dynamics accounting all the aspects built in our model.

3.2. Self- versus forced quarantine

Fig. 4 shows the trade-off between self- and forced quarantine in diminishing the epidemic size. We set the self-quarantine effort rate to 1 (100%) in the first column, but varied the forced quarantine rate to 30%, 50%, and 70%. The

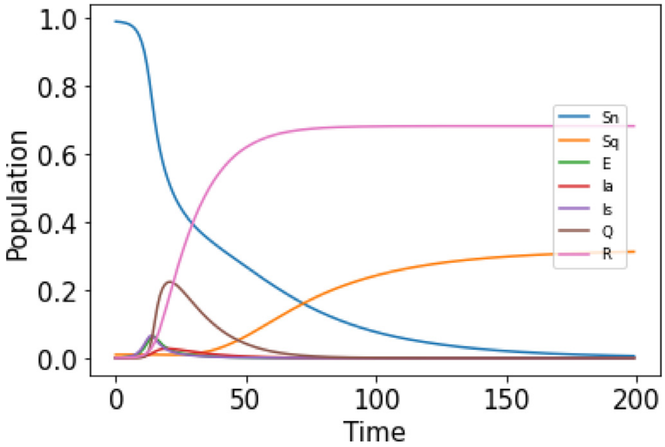

Fig. 3. Time-series for all compartments. The blue curve depicts susceptible people acting normally; the orange curve depicts susceptible people who have self-quarantined themselves; and the brown curve depicts people who have been infected and forced quarantined by the government at time *t*. The final epidemic size is determined by the pink curve. The green, red, violet curves represent the exposed, asymptomatic infected, and symptomatic infected patients, respectively. Here, all the parameters are taken as the standard one from Table 2.

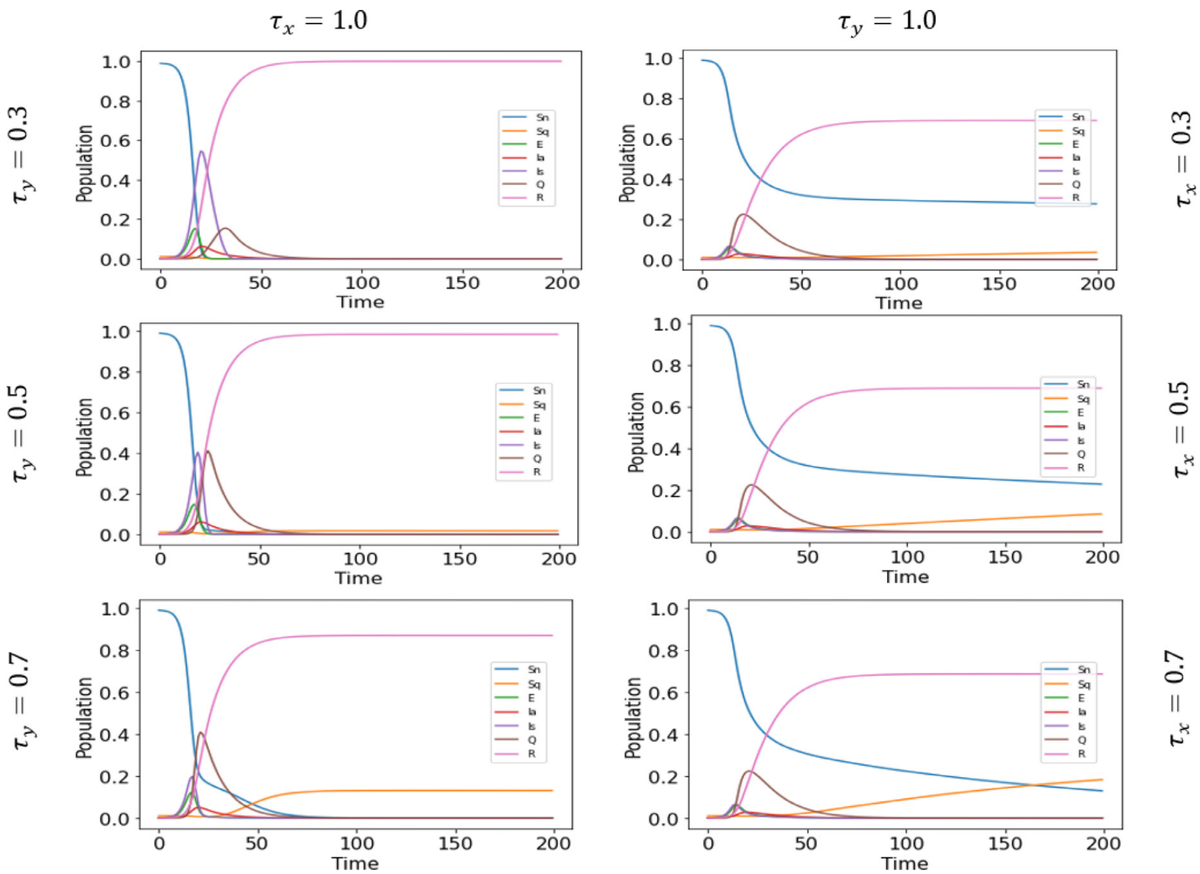

Fig. 4. The entire population's time series is depicted in this graph by adjusting the self-quarantine and forced quarantine effort rates. The other parameters and initial values are left at their default settings (Fig. 3). In the three graphs of first column, τ_x is fixed as 1, and $\tau_y$varies with 0.3, 0.5, 0.7, respectively. Similarly, in the second column, τ_y is fixed as 1, but τ_x varies with 0.3, 0.5, 0.7, respectively. In the first column, we can see that increasing the governmental effort can reduce the infection peak, whereas in the second column a proactive intervention by the government ($\tau_y = 1.0$) indirectly influence people to adhere to the voluntary self-provision (orange colored line in the second column). Also, a higher sensitivity (i.e., higher τ_x) increases the proportion of self-quarantined individuals.

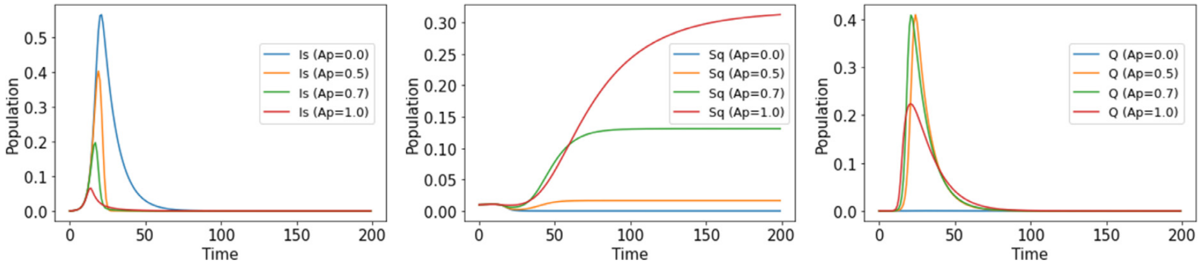

Fig. 5. Time series of symptomatic infected people (I_s), self-quarantine people (S_Q) and forced quarantine people (Q) are shown by varying the government total budget A_p from 0 to 1 where all the remaining parameters are taken as standard case.

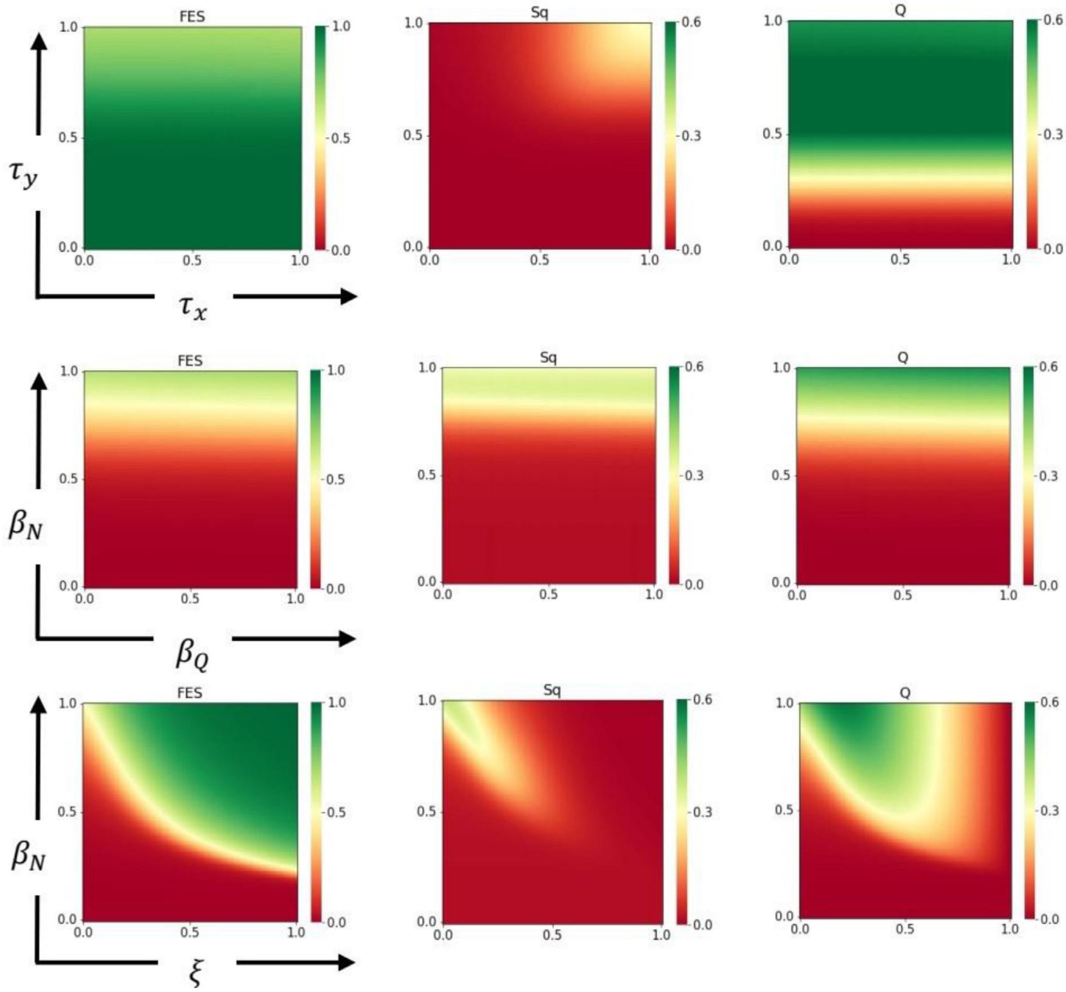

Fig. 6. Heatmaps of FES, $\sum S_Q$, $\sum Q$. Three different types of heatmaps are shown in each of the three rows. In the first column, FES is represented by a color bar ranging from 0 to 1. In the second and third columns, time-integrated self-quarantined and time-integrated forced quarantined people are represented by a color bar ranging from 0 to 0.6. In the first row, the panels are displayed by varying τ_x and τ_y from 0 to 1. The remaining parameters are set fixed with the standard ones. Similarly, in rows 2 and 3, the panels are displayed by varying β_Q and β_N, ξ and β_N from 0 to 1. Apparently, τ_y plays the pivotal role in reducing FES. Also, the fraction of self-conscious individuals (S_q) increases with β_N (second heatmap in the second row) although it does not improve the epidemic scenario as the self-provision is not perfect (first heatmap in the second row).

results illustrate that as the forced quarantine effort rate increases, the ultimate epidemic size decreases steadily, and it reduces to its smallest when the effort rate is 100%. The forced quarantine, in contrast to the self-provision, also reduces the peak epidemic size (see the first column in Fig. 4). In the second column, we varied the self-quarantine effort while keeping the maximum forced quarantine rate at 1. It is worth noting that as the self-quarantine effort was increased, more people moved from the S_N stage to the S_Q stage, meaning that people's awareness is growing aiding the epidemic management.

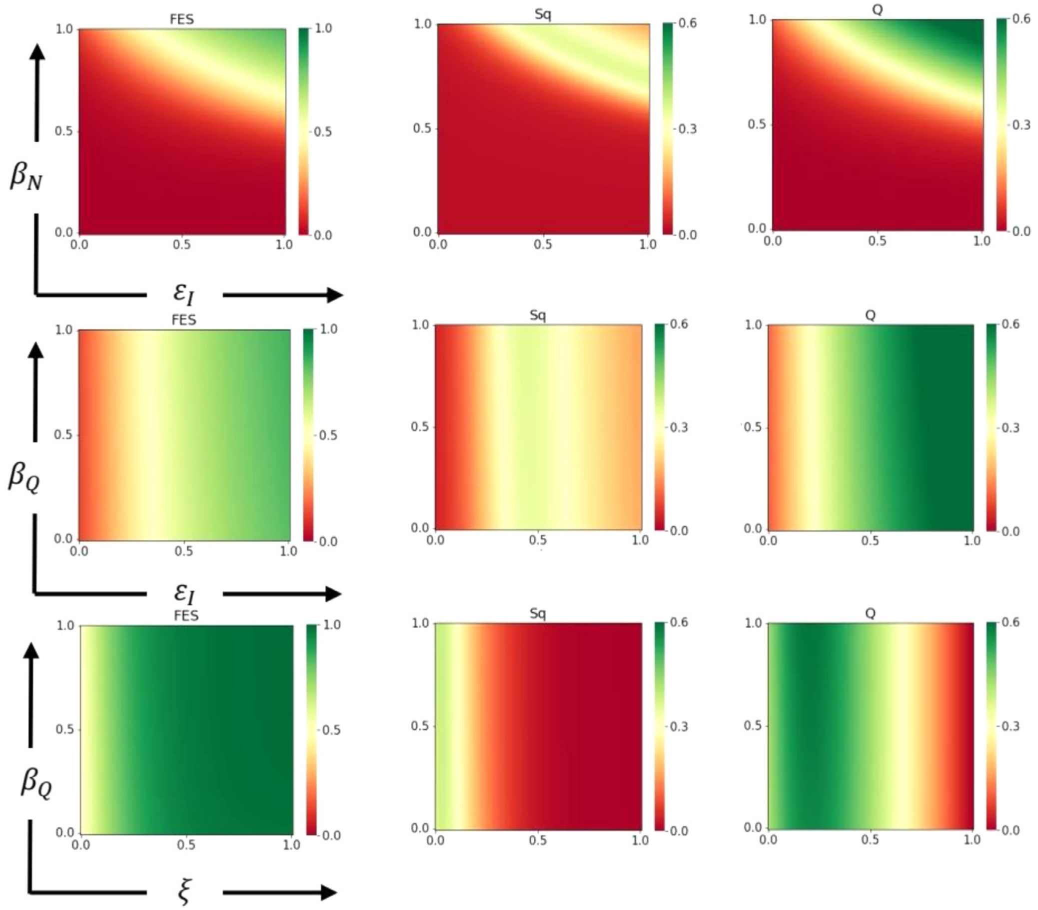

Fig. 7. Heatmaps of FES, $\sum S_Q$, $\sum Q$. In each of the three rows, three different kinds of heatmaps are displayed. A color bar ranging from 0 to 1 represents FES in the first column. A color bar ranging from 0 to 0.6 is used in the second and third columns to represent time-integrated self-quarantined and time-integrated forced quarantined people. In the first row, the panels are displayed by varying ε_I and β_N from 0 to 1. The remaining parameters are set fixed with the standard ones. Similarly, from rows 2 to 3, the panels are displayed by varying ε_I and β_Q, ξ and β_Q, respectively, from 0 to 1.

3.3. Varying the governmental total budget

Fig. 5 shows time evolution of the symptomatic infected, self-quarantined, and forced quarantined individuals. We demonstrate the results by varying the governmental budget. In the first graph, we see that increasing of the budget reduces the peak size of symptomatic infected people. If the budget is kept at minimum level meaning that if there is no governmental intervention, the peak of infected people occurs around 0.6, i.e., 60% of the total population can be infected. Increasing the budget can successively reduce the peak of the infected people because government can provide more facility. In second graph, increasing the total budget also increases the self-quarantine people as people are motivated from government to increase themselves for committing self-quarantine more. In the third graph, we can see that increasing of budget also increases the people in forced quarantine but, as self-quarantine increases there is less necessity to make people forced quarantined because the infected people are reduced due to conforming self-quarantine. Thus, forced quarantine is reduced with increasing the budget at maximum level.

3.4. Final epidemic size, time accumulated self-quarantine, time accumulated forced quarantine

In this section, we show some heatmaps (Figs. 6–8) of FES, time-integrated self-quarantine, and time-integrated forced quarantine when the parameters that primarily contribute to the basic reproduction number are varied. We also justify our parameter assumptions. We modify two parameters in each graph, while the remaining values are fixed according to our standard assumption.

As shown in Fig. 6, row (1), we can see that raising τ_y reduces FES while increasing τ_x has no effect on FES. We can also observe that increasing τ_x and τ_y sends more person into the self-quarantine condition. Increasing τ_y also causes more people to be forced into quarantine.

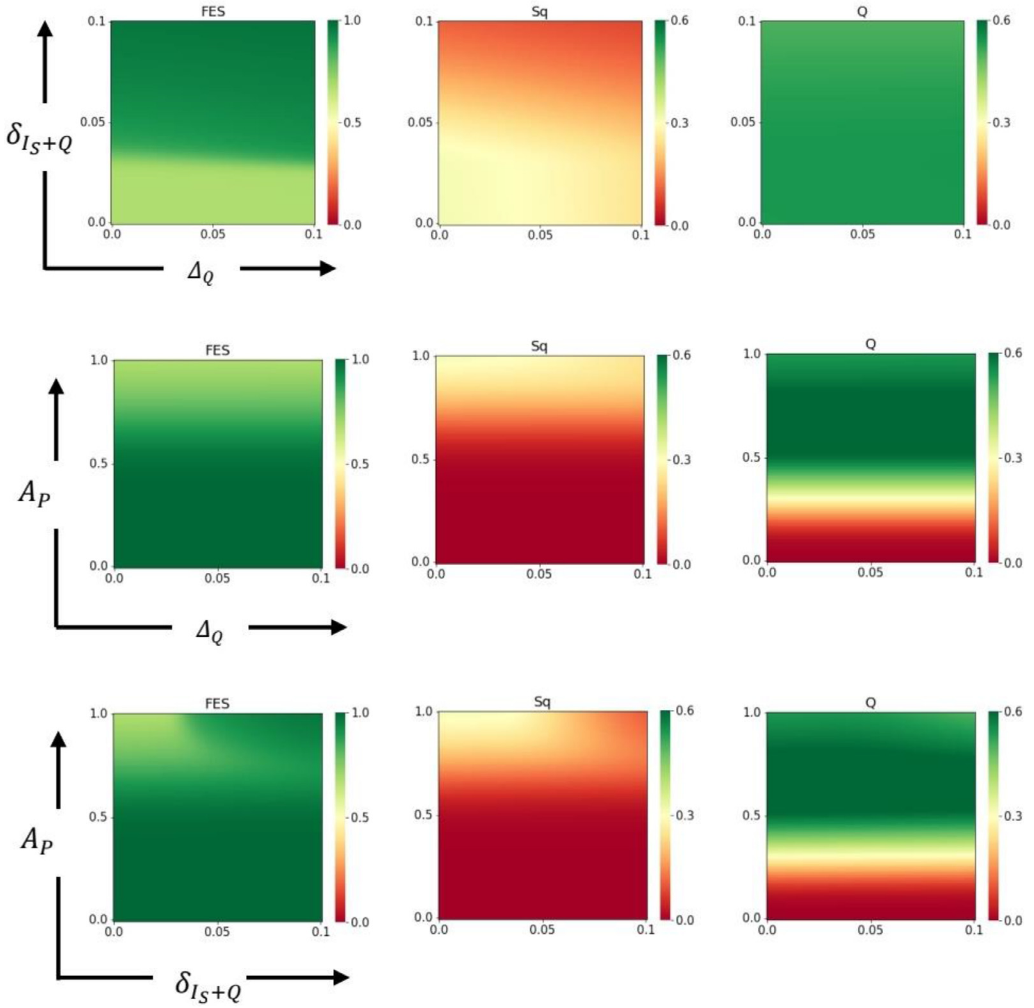

Fig. 8. Heatmaps of FES, $\sum S_Q$, $\sum Q$. Each of the three rows contains three different types of heatmaps. A color bar ranging from 0 to 1 represents FES. A color bar ranging from 0 to 0.6 represents time-integrated self-quarantined and time-integrated forced quarantined people in the second and third columns, respectively. In the first row, the panels are displayed by varying Δ_Q and δ_{I_S+Q} from 0 to 0.1. The remaining parameters are set fixed with the standard ones. Similarly, from rows 2 to 3, the panels are displayed by varying Δ_Q and A_P, δ_{I_S+Q} and A_P where Δ_Q and δ_{I_S+Q} vary from 0 to 0.1 and A_P varies from 0 to 1.

In row (2), the disease transmission rate from normal acting people, β_N, must be close to 1 to notice any influence on FES, whereas the diseases transmission rate from the self-quarantined people, β_Q, can be set anywhere from 0 to 1.

In row (3), the asymptomatic infection rate, ξ, should be lower to keep people in the self-quarantine and forced quarantine states. Increasing ξ makes the FES larger.

In rows (1–3) of Fig. 7, increasing the contact discount factor for asymptomatic people ε_I increases the FES. Like previous panels of Fig. 5, setting β_Q from 0 to 1 does not have any significant impact on the FES. Increasing of ξ can increase FES which is also observed in the previous panels of Fig. 6.

In row 1 of Fig. 8, increasing the self-quarantine cost for an individual from 0 to 0.1 does not have an impact on the reduction of FES but increasing the individual cost for forced quarantine greater than 0.03 significantly increases the value of FES. Additionally, the government's total budget needs to be set greater or equal to 1 (rows 2 and 3) to reduce the FES.

These results, Figs. 6–8 confirm the sensitivities from major model parameters on FES and total amount of quarantine individuals, which seems quite plausible.

3.5. ΔFES and critical points

In this section, we show (Fig. 9) the previously defined critical points and their consecutive lines, as well as the ΔFES in terms of the two cost parameters. In the region below the critical line, the total cost for self-quarantine and forced

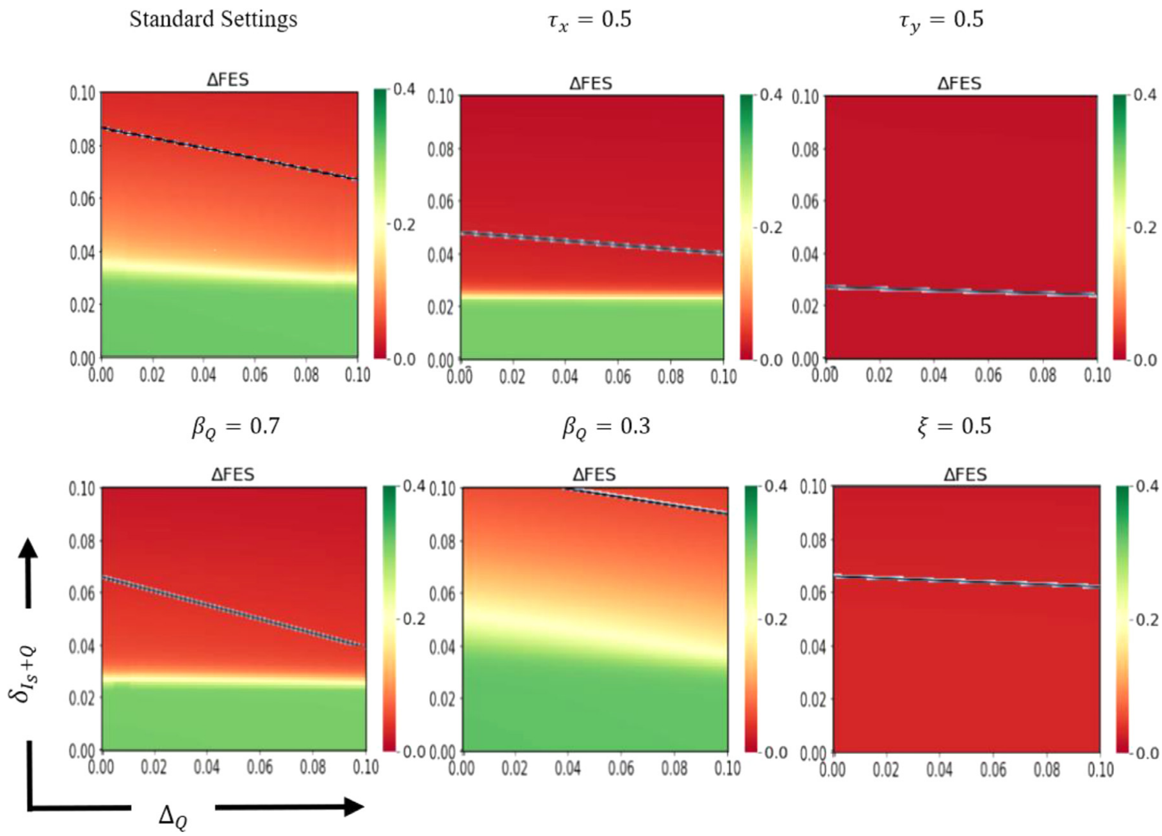

Fig. 9. ΔFES and critical lines are presented to observe the reduced cost margin using both interventions. In this figure, all panels represent the difference between FES with no intervention and FES with both interventions with a color bar ranging from 0 to 0.4 in terms of the individual cost parameters Δ_Q *and* δ_{I_S+Q}. All critical points are linked to form a line where the total cost of the epidemic equals the difference of two FES. With the standard set of parameters, ΔFES is represented in the first panel (upper leftmost) by green, yellow, and red zones, with moving from green to red indicating an increase in FES. Keeping the value of δ_{I_S+Q} less than 0.03, is the best option to make the government intervention more successful. The critical line marked the maximum value of cost combining the two total costs can be used to control the epidemic. It was observed that, for the first panel, when the self-quarantine cost for individual Δ_Q is zero the forced quarantine cost for individual δ_{I_S+Q} must be less than 0.087, and if $\Delta_Q = 0.1$, the maximum in our consideration, δ_{I_S+Q} must be less than 0.067. The remaining panels are presented by changing the other focal parameters (τ_x, τ_y, β_Q *and* ξ) of the model and observed the different values for Δ_Q *and* δ_{I_S+Q} to control the epidemic.

quarantine is less than the reduction of disease cost, indicating a favorable situation for cost-effective epidemic control by the two quarantine policies. When we reduce the self-quarantine effort (τ_x) by half (second panel of the first row), ΔFES decreases, implying less extent of reduction on FES by both interventions. Needless to say, it is a worse scenario than the standard settings. If we reduce the forced quarantine effort (τ_y) (third panel of the first row), the situation deteriorates even more than in the previous two cases. Increasing (first panel of the second row) and decreasing (second panel of the second row) β_Q results in a worse and better scenario than the standard case that is conceivable. As the rate of asymptomatic infection (ξ) rises (third panel of the second row), the situation worsens.

3.6. ASP and SED

Fig. 10 shows the heatmaps of FES, time-integrated S_Q, and time-integrated Q along the cost parameters for NE (row 1) and SO (row 2). In row 3, ASP^{NE} and ASP^{SO} are presented along with the SED for the standard set of parameters. Here, we observe that increasing the value of δ_{I_S+Q}brings higher FES (because of less incentive to quarantine), while increasing the value of Δ_Q has less effect on FES in NE. In SO, we can observe less FES because the maximum flux of $x = 1.0$ and $y = 1.0$ brings the minimum FES, and most people are moving to the S_Q state. Consequently, the ASP^{SO} is very close to zero. Thus, SED is similar to ASP^{NE}. We observe that increasing the value of δ_{I_S+Q} brings more positive value of SED; thus, the social dilemma increases.

Note that the SED is featured with a larger sensitivity in δ_{I_S+Q} direction than that in Δ_Q direction. It is paraphrased by the allegation that the government could solve a more severe social dilemma than that imposed on each individual around

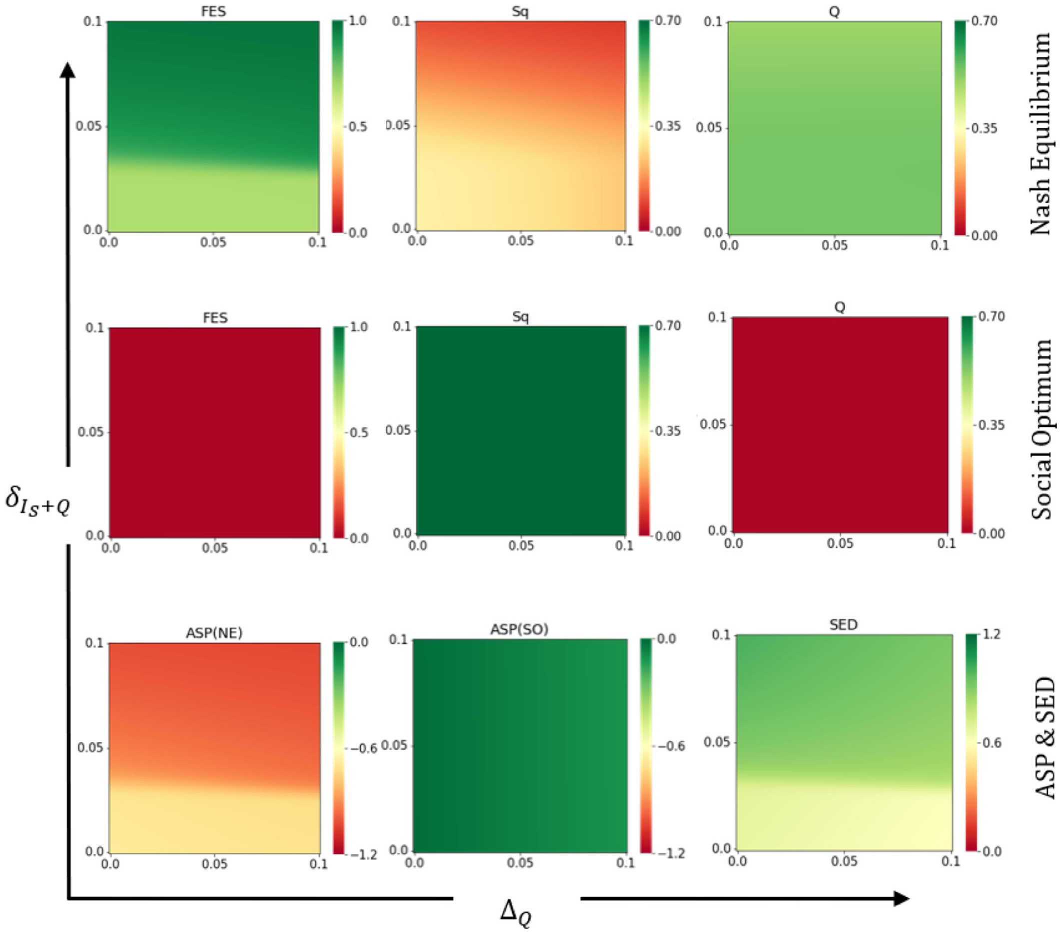

Fig. 10. FES, $\sum S_Q$, $\sum Q$, ASP at NE, SO, and SED to observe the social dilemma. In this figure, the FES, time-integrated S_Q, and time-integrated Q are represented in the first two rows for the case of Nash equilibrium and social optimum in terms of the cost parameters Δ_Q *and* δ_{I_S+Q}. FES panels are displayed with a color bar ranging from 0 to 1, whereas S_Q and Q panels are displayed with a color bar ranging from 0 to 0.7. In the third row, ASP at NE and SO are displayed with a color bar ranging from − 1.2 to 0.0, and SED is displayed with a color bar ranging from 0.0 to 1.2. Apparently, the governmental intervention cost seems more influential in reducing the disease prevalence and social efficiency deficit.

whether he/she is committing self-quarantine by increasing the government's effort to let more infected individuals forcefully quarantined. Thus, the social dilemma acting on the government level (through the provision of forced quarantine) is more severe than another social dilemma acting on an individual level (around self-quarantine). This is because governmental intervention through forced quarantine is more effective oppressing disease from spreading. This fact might be conceivable because self-quarantine works in an 'ex-post' way where infected people who quarantine never get infected again (they must stay at Q; see Fig. 1). However, self-quarantine only works as pre-emptive; an individual once self-quarantined may (may not) get infected sooner or later.

Fig. 11 shows some other combinations for ASP^{NE} and corresponding SED. For the first case (1st and 3rd panels of row 1), if $\tau_x = 0.5$, i.e., the effort rate of self-quarantine is reduced, then ASP^{NE} and SED almost behave the same with the standard case, meaning that increasing the forced quarantine costs for individual increases the social dilemma. However, if τ_y is reduced (2nd and 4th panels of row 1), ASP^{NE} is getting lower brings SED higher; thus, so the social dilemma increases more than the standard case, which is not an ideal situation to control the epidemic. If the transmission rate β_Q reduces (1st and 3rd panels of row 2), more people stay in the S_Q state, resulting in a dilemma that reduces more than the standard case. Similarly increasing β_Q (2nd and 4th panels of row 2) increases the value of FES, and more people are going to be infected; thus, reducing reduces the dilemma more than the standard case. If the asymptomatic infection rate (ξ) increased (row 3), FES also increased, and the value of SED gets closer to zero, meaning that there is no dilemma when most of the people are asymptomatic.

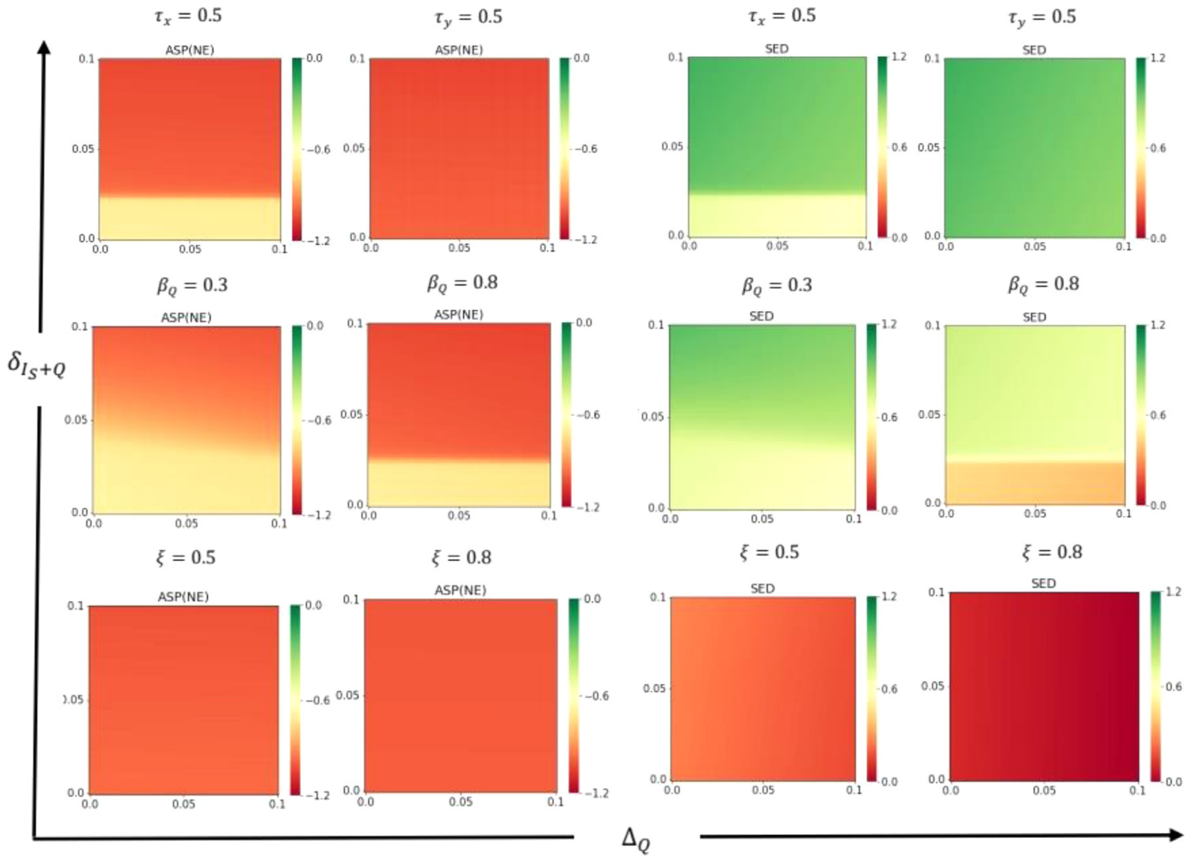

Fig. 11. ASP at NE and corresponding SED to observe the social dilemma. In this figure, different ASPs at NE are displayed along with the corresponding SED with a color bar ranging from − 1.2 to 0.0 and 0.0 to 1.2, respectively. All panels are drawn in terms of the cost parameters Δ_Q *and* δ_{I_S+Q}.

4. Conclusion

In this study, we developed an epidemiological model based on SEIR dynamics that considers dynamic human behavior for individuals and governments regarding self-quarantine and forced quarantine, respectively. The aim was to observe the interplay between both provisions towards controlling disease spreading. In general, imposing compulsory quarantine by the government seems more effective in containing the disease than self-quarantine. We also demonstrated that increasing the government's compulsory quarantine rate can considerably reduce the value of the basic reproduction number. Additionally, we observed that a proactive authoritative measure (quantified by a higher sensitivity to forced quarantine) upsurges the fraction of self-quarantine (Fig. 4), which intuitively indicates that the government's increased effort made people more aware of the importance of self-quarantine. In terms of cost parameters, we observed that the government must keep the cost of forced quarantine under control, whereas the cost of self-quarantine does not need to be regulated.

We further demonstrated the impact of both provisions in reducing the social efficiency deficit, which is quantified by the gap between the overall payoff at social optimum and at equilibrium. Our results suggest that authoritative intervention (i.e., forced quarantine) is more effective to reduce such deficit. The analysis of SED reveals that there are rich and complex dynamics depending on the cost of forced quarantine of individuals, but not so much for the cost of self-quarantine for individuals. Also, by observing the features at NE with the prediction of our behavior model, human decisions have an inertial influence which allows humans to take certain preventive measures to slow the disease from spreading.

We intend to expand our models in the future. We might add a vaccine compartment, where people can choose their immunization to limit the danger of a pandemic. The government should focus on overall vaccination coverage to lower the death rate. We are also looking into how the inclusion of multi-strain epidemic models affects social behavior, such as self-quarantine or vaccination.

Data Availability

Data will be made available on request.

Acknowledgments

This study was partially supported by Grant-in-Aid for Scientific Research from JSPS, Japan, KAKENHI (Grant No. JP 19KK0262, JP 20H02314, and JP 20K21062) awarded to Professor Tanimoto. We would like to express our gratitude to them.

References

[1] M. Alam, K.M.A. Kabir, J. Tanimoto, Based on mathematical epidemiology and evolutionary game theory, which is more effective: quarantine or isolation policy, J. Stat. Mech. Theory Exp. (2020) 2020, doi:10.1088/1742-5468/ab75ea.
[2] N. Nkire, K. Mrklas, M. Hrabok, A. Gusnowski, W. Vuong, S. Surood, A. Abba-Aji, L. Urichuk, B. Cao, A.J. Greenshaw, V.I.O. Agyapong, COVID-19 pandemic: demographic predictors of self-isolation or self-quarantine and impact of isolation and quarantine on perceived stress, Anxiety Depression Front. Psychiatry. 12 (2021) 1–8, doi:10.3389/fpsyt.2021.553468.
[3] M.S. Aronna, R. Guglielmi, L.M. Moschen, A model for COVID-19 with isolation, quarantine and testing as control measures, Epidemics 34 (2021) 100437, doi:10.1016/j.epidem.2021.100437.
[4] C.R. Wells, P. Sah, S.M. Moghadas, A. Pandey, A. Shoukat, Y. Wang, Z. Wang, L.A. Meyers, B.H. Singer, A.P. Galvani, Impact of international travel and border control measures on the global spread of the novel 2019 coronavirus outbreak, Proc. Natl. Acad. Sci. U. S. A. 117 (2020) 7504–7509, doi:10.1073/pnas.2002616117.
[5] I. Yen-Hao Chu, P. Alam, H.J. Larson, L. Lin, Social consequences of mass quarantine during epidemics: a systematic review with implications for the COVID-19 response, J. Travel Med. 27 (2020) 1–14, doi:10.1093/JTM/TAAA192.
[6] D. Meidan, N. Schulmann, R. Cohen, S. Haber, E. Yaniv, R. Sarid, B. Barzel, Alternating quarantine for sustainable epidemic mitigation, Nat. Commun. 12 (2021) 1–12, doi:10.1038/s41467-020-20324-8.
[7] G. De Meijere, V. Colizza, E. Valdano, C. Castellano, Effect of delayed awareness and fatigue on the efficacy of self-isolation in epidemic control, Phys. Rev. E. 104 (2021) 1–8, doi:10.1103/PhysRevE.104.044316.
[8] K.M.A. Kabir, T. Risa, J. Tanimoto, Prosocial behavior of wearing a mask during an epidemic: an evolutionary explanation, Sci. Rep. 11 (2021) 1–14, doi:10.1038/s41598-021-92094-2.
[9] M.A. Amaral, M.M. d. Oliveira, M.A. Javarone, An epidemiological model with voluntary quarantine strategies governed by evolutionary game dynamics, Chaos Solitons Fractals 143 (2021) 110616, doi:10.1016/j.chaos.2020.110616.
[10] K.A. Kabir, A. Chowdhury, J. Tanimoto, An evolutionary game modeling to assess the effect of border enforcement measures and socio-economic cost: Export-importation epidemic dynamics, Chaos Solitons Fractals 146 (2021) 110918, doi:10.1016/j.chaos.2021.110918.
[11] W. Adiyoso, Wilopo, Social distancing intentions to reduce the spread of COVID-19: The extended theory of planned behavior, BMC Public Health 21 (2021) 1–12, doi:10.1186/s12889-021-11884-5.
[12] A. Chowdhury, K.M.A. Kabir, J. Tanimoto, How quarantine and social distancing policy can suppress the outbreak of novel coronavirus in developing or under poverty level countries: a mathematical and statistical analysis, Biometrics Biostat. Int. J. 10 (2020) 145–152, doi:10.21203/rs.3.rs-20294/v1.
[13] A. Aleta, D. Martín-Corral, A. Pastore y Piontti, M. Ajelli, M. Litvinova, M. Chinazzi, N.E. Dean, M.E. Halloran, I.M. Longini, S. Merler, A. Pentland, A. Vespignani, E. Moro, Y. Moreno, Modelling the impact of testing, contact tracing and household quarantine on second waves of COVID-19, Nat. Hum. Behav. 4 (2020) 964–971, doi:10.1038/s41562-020-0931-9.
[14] M. Jusup, P. Holme, K. Kanazawa, M. Takayasu, I. Romić, Z. Wang, S. Geček, T. Lipić, B. Podobnik, L. Wang, W. Luo, T. Klanjšček, J. Fan, S. Boccaletti, M. Perc, Social physics, Phys. Rep. 948 (2022) 1–148, doi:10.1016/j.physrep.2021.10.005.
[15] D. Helbing, D. Brockmann, T. Chadefaux, K. Donnay, U. Blanke, O. Woolley-Meza, M. Moussaid, A. Johansson, J. Krause, S. Schutte, M. Perc, Saving human lives: what complexity science and information systems can contribute, 2015. https://doi.org/10.1007/s10955-014-1024-9.
[16] T. Lee, H.D. Kwon, J. Lee, The effect of control measures on COVID-19 transmission in South Korea, PLoS One 16 (2021) 1–18, doi:10.1371/journal.pone.0249262.
[17] J. Tanimoto, Fundamentals of evolutionary game theory and its applications, Springer, Tokyo, 2015.
[18] J. Tanimoto, Sociophysics approach to epidemics, Springer, Tokyo, 2021.
[19] J. Tanimoto, Evolutionary games with sociophysics: Analysis of traffic flow and epidemics, Springer, Tokyo, 2019.
[20] A. Babaei, M. Ahmadi, H. Jafari, A. Liya, A mathematical model to examine the effect of quarantine on the spread of coronavirus, Chaos Solitons Fractals 142 (2021) 33–37, doi:10.1016/j.chaos.2020.110418.
[21] G. Pietrabissa, S.G. Simpson, Psychological Consequences of Social Isolation During COVID-19 Outbreak, Front. Psychol. 11 (2020) 9–12, doi:10.3389/fpsyg.2020.02201.
[22] V. Nenchev, Optimal quarantine control of an infectious outbreak, Chaos Solitons Fractals 138 (2020) 110139, doi:10.1016/j.chaos.2020.110139.
[23] C.E. Madubueze, S. Dachollom, I.O. Onwubuya, Controlling the spread of COVID-19: optimal control analysis, Comput. Math. Methods Med. (2020) 2020, doi:10.1155/2020/6862516.
[24] K.M. Ariful Kabir, M. Jusup, J. Tanimoto, Behavioral incentives in a vaccination-dilemma setting with optional treatment, Phys. Rev. E. 100 (2019) 1–13, doi:10.1103/PhysRevE.100.062402.
[25] M. Ahsan Habib, M. Tanaka, J. Tanimoto, How does conformity promote the enhancement of cooperation in the network reciprocity in spatial prisoner's dilemma games? Chaos Solitons Fractals 138 (2020) 109997, doi:10.1016/j.chaos.2020.109997.
[26] M.R. Arefin, J. Tanimoto, Evolution of cooperation in social dilemmas under the coexistence of aspiration and imitation mechanisms, Phys. Rev. E. 102 (2020) 32120, doi:10.1103/PhysRevE.102.032120.
[27] J. Tanimoto, H. Sagara, Relationship between dilemma occurrence and the existence of a weakly dominant strategy in a two-player symmetric game, BioSystems 90 (2007) 105–114, doi:10.1016/j.biosystems.2006.07.005.
[28] K.M. Ariful Kabir, J. Tanimoto, Modelling and analysing the coexistence of dual dilemmas in the proactive vaccination game and retroactive treatment game in epidemic viral dynamics, Proc. R. Soc. A Math. Phys. Eng. Sci. (2019) 475, doi:10.1098/rspa.2019.0484.
[29] M.R. Arefin, K.M.A. Kabir, M. Jusup, H. Ito, J. Tanimoto, Social efficiency deficit deciphers social dilemmas, Sci. Rep. 10 (2020) 1–9, doi:10.1038/s41598-020-72971-y.
[30] A. Szolnoki, M. Perc, Conformity enhances network reciprocity in evolutionary social dilemmas, J. R. Soc. Interface. 12 (2015) 2–9, doi:10.1098/rsif.2014.1299.
[31] C. Ohajunwa, K. Kumar, P. Seshaiyer, Mathematical modeling, analysis, and simulation of the COVID-19 pandemic with explicit and implicit behavioral changes, Comput. Math. Biophys. 8 (2020) 216–232, doi:10.1515/cmb-2020-0113.
[32] U. Foryś, Mathematical models in epidemiology and immunology, 2000. https://doi.org/10.14708/ma.v28i42/01.1879.
[33] D. Stipic, M. Bradac, T. Lipic, B. Podobnik, Effects of quarantine disobedience and mobility restrictions on COVID-19 pandemic waves in dynamical networks, Chaos Solitons Fractals 150 (2021) 111200, doi:10.1016/j.chaos.2021.111200.
[34] M.A. Safi, A.B. Gumel, Dynamics of a model with quarantine-adjusted incidence and quarantine of susceptible individuals, J. Math. Anal. Appl. 399 (2013) 565–575, doi:10.1016/j.jmaa.2012.10.015.
[35] M.A. Safi, A.B. Gumel, The effect of incidence functions on the dynamics of a quarantine/isolation model with time delay, Nonlinear Anal. Real World Appl. 12 (2011) 215–235, doi:10.1016/j.nonrwa.2010.06.009.
[36] M.U.G. Kraemer, C.H. Yang, B. Gutierrez, C.H. Wu, B. Klein, D.M. Pigott, L. du Plessis, N.R. Faria, R. Li, W.P. Hanage, J.S. Brownstein, M. Layan, A. Vespignani, H. Tian, C. Dye, O.G. Pybus, S.V. Scarpino, The effect of human mobility and control measures on the COVID-19 epidemic in China, Science (80-.) 368 (2020) 493–497, doi:10.1126/science.abb4218.

[37] K.M.A. Kabir, J. Tanimoto, Evolutionary game theory modelling to represent the behavioural dynamics of economic shutdowns and shield immunity in the COVID-19 pandemic: Economic shutdowns and shield immunity, R. Soc. Open Sci. 7 (2020), doi:10.1098/rsos.201095rsos201095.
[38] K.M.A. Kabir, K. Kuga, J. Tanimoto, Analysis of SIR epidemic model with information spreading of awareness, Chaos Solitons Fractals 119 (2019) 118–125, doi:10.1016/j.chaos.2018.12.017.
[39] M. Martcheva, An introduction to mathematical epidemiology, 2013.
[40] C.T. Deressa, Y.O. Mussa, G.F. Duressa, Optimal control and sensitivity analysis for transmission dynamics of Coronavirus, Results Phys. 19 (2020) 103642, doi:10.1016/j.rinp.2020.103642.
[41] K. Miyaji, J. Tanimoto, A co-evolutionary model combined mixed-strategy and network adaptation by severing disassortative neighbors promotes cooperation in prisoner's dilemma games, Chaos Solitons Fractals 143 (2021) 110603, doi:10.1016/j.chaos.2020.110603.
[42] Z. Feng, Final and peak epidemic sizes for seir models, Math. Biosci. Eng. 4 (2007) 675–686.
[43] T. Hussain, M. Ozair, F. Ali, S. ur Rehman, T.A. Assiri, E.E. Mahmoud, Sensitivity analysis and optimal control of COVID-19 dynamics based on SEIQR model, Results Phys 22 (2021) 103956, doi:10.1016/j.rinp.2021.103956.
[44] J. Fan, Q. Yin, C. Xia, M. Perc, Epidemics on multilayer simplicial complexes, Proc. R. Soc. A Math. Phys. Eng. Sci. (2022) 478, doi:10.1098/rspa.2022.0059.
[45] H.J. Li, W. Xu, S. Song, W.X. Wang, M. Perc, The dynamics of epidemic spreading on signed networks, Chaos Solitons Fractals 151 (2021) 111294, doi:10.1016/j.chaos.2021.111294.
[46] C.T. Bauch, Imitation dynamics predict vaccinating behaviour, Proc. R. Soc. B Biol. Sci. 272 (2005) 1669–1675, doi:10.1098/rspb.2005.3153.
[47] C.T. Bauch, S. Bhattacharyya, Evolutionary game theory and social learning can determine how vaccine scares unfold, PLoS Comput. Biol. 8 (2012), doi:10.1371/journal.pcbi.1002452.
[48] A. Deka, S. Bhattacharyya, The effect of human vaccination behaviour on strain competition in an infectious disease: An imitation dynamic approach, Theor, Popul. Biol. 143 (2022) 62–76, doi:10.1016/j.tpb.2021.12.001.
[49] M.R. Arefin, T. Masaki, J. Tanimoto, Vaccinating behaviour guided by imitation and aspiration: vaccinating behav. - Imit. And asp, Proc. R. Soc. A Math. Phys. Eng. Sci. (2020) 476, doi:10.1098/rspa.2020.0327rspa20200327.
[50] M.R. Arefin, K.M.A. Kabir, J. Tanimoto, A mean-field vaccination game scheme to analyze the effect of a single vaccination strategy on a two-strain epidemic spreading, J. Stat. Mech. Theory Exp. (2020) 2020, doi:10.1088/1742-5468/ab74c6.
[51] M.R. Arefin, J. Tanimoto, Imitation and aspiration dynamics bring different evolutionary outcomes in feedback-evolving games, Proc. R. Soc. A Math. Phys. Eng. Sci. (2021) 477, doi:10.1098/rspa.2021.0240.
[52] J.K. Taubenberger, D.M. Morens, 1918 influenza: the mother of all pandemics, Emerg. Infect. Dis. 12 (2006) 15–22, doi:10.3201/eid1209.050979.
[53] E. Schneider, Severe acute respiratory syndrome (SARS), Netter's Infect. Dis. (2012) 537–543, doi:10.1016/B978-1-4377-0126-5.00089-6.
[54] R. Tori, J. Tanimoto, A study on prosocial behavior of wearing a mask and self-quarantining to prevent the spread of diseases underpinned by evolutionary game theory, Chaos, Solitons Fractals Interdiscip, J. Nonlinear Sci. Nonequilibrium Complex Phenom. 158 (2022) 112030, doi:10.1016/j.chaos.2022.112030.
[55] O. Diekmann, J.A.P. Heesterbeek, J.A.J. Metz, On the definition and the computation of the basic reproduction ratio R0 in models for infectious diseases in heterogeneous populations, J. Math. Biol. 28 (1990) 365–382, doi:10.1007/BF00178324.
[56] D. Niño-Torres, A. Ríos-Gutiérrez, V. Arunachalam, C. Ohajunwa, P. Seshaiyer, Stochastic modeling, analysis, and simulation of the COVID-19 pandemic with explicit behavioral changes in Bogotá: a case study, Infect. Dis. Model. 7 (2022) 199–211, doi:10.1016/j.idm.2021.12.008.